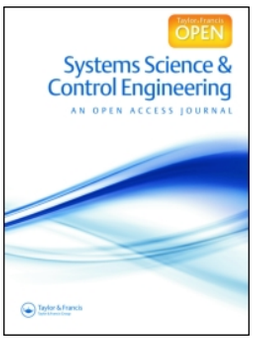

Taylor & Francis
Taylor & Francis Group

Systems Science & Control Engineering

An Open Access Journal

ISSN: (Print) 2164-2583 (Online) Journal homepage: https://www.tandfonline.com/loi/tssc20

Optimised PID control for tilting trains

F. Hassan, A. C. Zolotas & R. M. Margetts

To cite this article: F. Hassan, A. C. Zolotas & R. M. Margetts (2017) Optimised PID control for tilting trains, Systems Science & Control Engineering, 5:1, 25-41, DOI: 10.1080/21642583.2016.1275990

To link to this article: https://doi.org/10.1080/21642583.2016.1275990

Published online: 13 Jan 2017.

SYSTEMS SCIENCE & CONTROL ENGINEERING: AN OPEN ACCESS JOURNAL, 2017
VOL. 5, NO. 1, 25–41
https://doi.org/10.1080/21642583.2016.1275990

Taylor & Francis
Taylor & Francis Group

Optimised PID control for tilting trains

F. Hassan, A. C. Zolotas and R. M. Margetts

School of Engineering, College of Science, University of Lincoln, Lincoln, UK

ABSTRACT

Nulling-type tilt control in tilting railway vehicles, i.e. Single-Input–Single-Output (SISO) control using non-precedent sensor information for lateral acceleration and tilt angle, suffers from performance limitations due to the system's non-minimum phase characteristics [Zolotas, A. C., & Goodall, R. M. (2000). *Advanced control strategies for tilting railway vehicles*. UKACC international conference on control, University of Cambridge, Cambridge, UK. 6p., ISBN: 0-85296-240-1.]. From an engineering point of view, this is due to the suspension's dynamic interactions and the sensor information used for feedback control. This paper revisits SISO PID-based nulling-type tilt control design (hereby referred to as 'economical tilt control') and rigorously studies its design via optimization to improve system performance. The strong coupling between the roll and lateral dynamic modes of the vehicle body is shown and the performance limitations using conventional control highlighted. PID controllers are designed to illustrate different levels of tilt performance regarding the deterministic (curving acceleration response) and stochastic (ride quality) with the latter being a bounded constraint. With novel contribution to use of PID control in the tilt control application with rational transfer functions, particular emphasis is placed on the practical aspects of the tilt dynamics within the design framework via detailed simulation results.

ARTICLE HISTORY
Received 12 December 2016
Accepted 20 December 2016

KEYWORDS
Active suspensions; PID control; optimization; ride quality; rail vehicles

1. Introduction

Tilting trains lean the body of the vehicle inwards on curves to reduce lateral acceleration experienced by passengers. Train speed increases through the curve, resulting in the reduction of journey times. From a practical viewpoint, active control is used to perform the tilting action and active tilting train systems is an area whereby control engineering has been a major contributor to modern train vehicle technology (Pearson, Goodall, & Pratt, 1998; Stribersky, Steidl, Müller, & Rath, 1996). Nowadays a large number of modern high-speed trains incorporate a form of tilt (Fröidh, 2008; Iwnicki, 2006; Vickerman, 1997).

Initial studies of tilting trains used what we refer to as a form of 'economical tilt control' (Huber, 1998) due to its single-input–single-output nature, i.e. feedback control from a single lateral accelerometer mounted on the body of the passenger vehicle. This early approach proved difficult to achieve sufficiently fast response on the curve transitions without causing a deterioration of ride quality on (straight) track misalignments. The trend nowadays is to use a command-driven system in which a signal from an accelerometer on a non-tilting part of the previous vehicle (or front passenger vehicle) commands the required tilting angle, with a straightforward tilt angle feedback controller locally ensuring that each vehicle tilts to the indicated tilt angle (Persson, Goodall, & Sasaki, 2009; Zolotas, Halikias, & Goodall, 2000). The above solution is commonly known as 'tilt with precedence', i.e. preview-tilt information from preview vehicle enables a sufficient level of filtering to be applied to remove the effect of track irregularities on the tilt command signal. Although this approach is the currently accepted industrial practice in tilt systems, it can be a complex overall scheme; amongst other things it must be reconfigured when the train changes direction, and it is also difficult to provide a satisfactory performance for the leading vehicle of the train. It is worth noting that GPS systems, including track database information are used in some cases although still issues of signal, quality communication, delays, and tunnels may affect operation and adding further complexity (Bruni, Goodall, Mei, & Tsunashima, 2007; Huber, 1998; Pearson et al., 1998). Tilting trains continue evolving in terms of structure and tilt mechanisms (Colombo, Di Gialleonardo, Facchinetti, & Bruni, 2014; Shinmura, Hayashi, Okada, & Kamikawa, 2015) which undoubtedly facilitates further exploration of advanced control design.

A number of studies on tilt control exist (Pearson et al., 1998; Zamzuri, Zolotas, & Goodall, 2006a,

CONTACT A. C. Zolotas azolotas@lincoln.ac.uk, a.zolotas@ieee.org

2006b, 2008; Zhou, Zolotas, & Goodall, 2013; Zolotas et al., 2000), although no study has yet rigorously investigated advanced classical PID control via optimization – of relative to tilt control interest – cost functions. The paper by Zamzuri et al. (2006b) employed ITAE (Integral of Time Multiply Absolute Error) and Z-N (Ziegler–Nichols) from a fuzzy PID-tilt point of view, while earlier work by Pearson et al. (1998) looked at both classical and optimal control from a practical viewpoint of limited tilt for a practical ARB (anti-roll bar) tilt vehicle. In addition, there are numerous papers discussing multivariable control for the tilt problem directly dealing with the complexity of the tilt control design but – naturally – not studying details of classical baseline control, i.e. Pearson et al. (1998), Zhou, Zolotas, and Goodall (2014), Zolotas, Goodall, and Halikias (2002) and Zhou, Zolotas, and Goodall (2010).

The present paper proposes, in a rigorous manner, optimized PID control design and the related impact on tilt control trade-off (tilt following vs. ride quality). We revisit earlier results on PID-type nulling-tilt control and report findings on advanced PID control via optimization tools. With novel contribution on the tilt application, the aim is twofold: (i) still opting for a simple classical control solution in the tilt suspension problem, (ii) to investigate the extend of improving tilt performance trade-off by tilt-targeted tuned PID controllers, and the controller ability to deal with the cumbersome deterministic/stochastic tilt performance issue. We study the capability of enhanced PID control to address the tilt control problem, and indirectly its usefulness as a potential baseline controller/filter in further advanced control study. It is worth noting that, in this paper, 'nulling-tilt' actually refers to 'partial-nulling-tilt ' control.

2. Vehicle modelling information and design preamble

2.1. Vehicle end-view

The end-view of a typical tilt across secondary (with anti-roll bar) train vehicle is shown in Figure 1. The mathematical representation of the ARB tilt model stems from the work presented in Zolotas, Wang, and Goodall (2008), but details of the dynamic equations used are included in Appendix 1 for completeness. It is worth noting that actuator (tilt command-to applied tilt relationship) position servo-dynamics have also been taken in account and is given by the following expression:

$$\ddot{\delta}_{(t)}(t) = -a^{-1}\dot{\delta}_{(t)}(t) + a^{-1}K_m k_a(\delta_{(ti)}(t) - \delta_{(t)}(t)). \quad (1)$$

In fact, this is included to incorporated realistic actuator bandwidth capability. Note that the actuator dynamics parameters are selected to provide damping of 50% and a bandwidth of 3.5 Hz (the usually expected dynamic behaviour in railway actuator systems).

In practice the model will have a form of nonlinear behaviour. However, a linearized version on a curved track is a good approximation for analysis and designing robust control. In this context, the overall roll angle from horizon (cant + expected tilt) is not to exceed 14–16°. The mathematical model (with equations presented in Appendix 1) can be arranged in the usual state-space

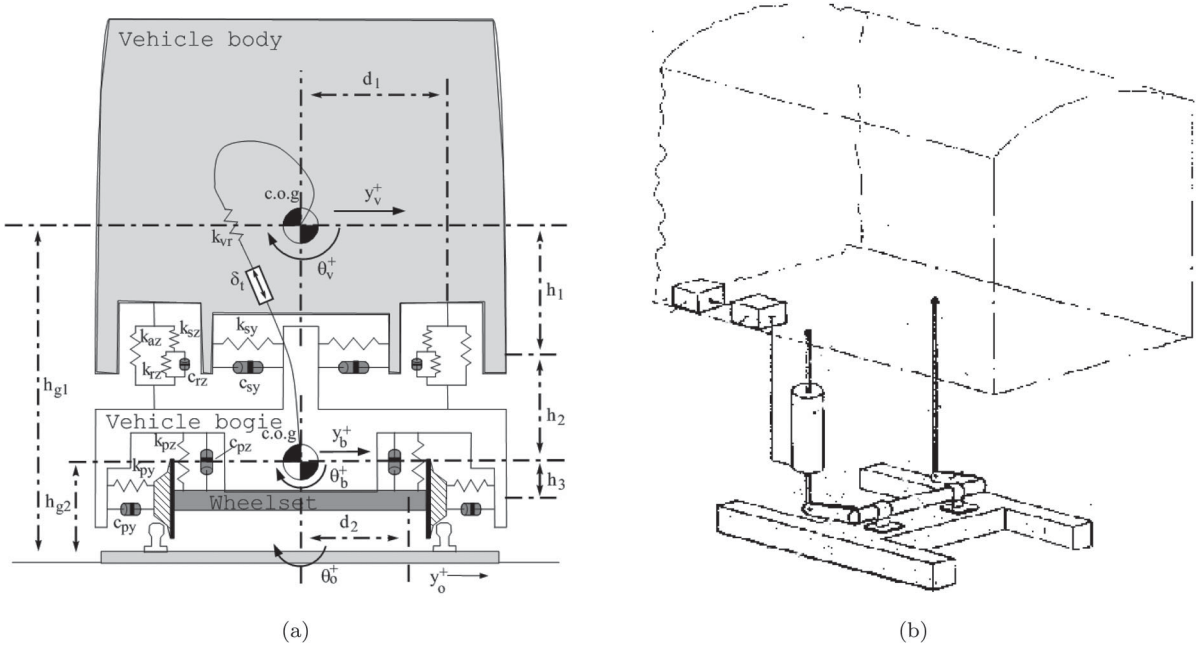

Figure 1. Tilting vehicle end-view. (a) End-view diagram and (b) Schematic of typical tilt across setup (ARB).

Table 1. Vehicle modal analysis for the ARB Tilt model.

Mode	Damping (%)	Frequency (Hz)
Body lower sway	16.5	0.67
Body upper sway	27.2	1.50
Bogie lateral	12.4	26.8
Bogie roll	20.8	11.1
Bogie Lateral kinematics (wheel set filtering)	20.0	5.00
Air spring	100.0	3.70
Actuator	50.0	3.50

form with state vector (Zolotas et al., 2008).

$$\dot{x}(t) = \mathbf{A}x(t) + \mathbf{B_u}u(t) + \mathbf{B_w}w(t). \tag{2}$$

With the state vector, control input and exogenous input vectors are – (t) dropped for simplicity

$$x = [y_v \ \theta_v \ y_b \ \theta_b \ \dot{y}_v \ \dot{\theta}_v \ \dot{y}_b \ \dot{\theta}_b \ \theta_r \ \delta_t \ \dot{\delta}_t \ y_w \ \dot{y}_w]^T, \tag{3}$$

$$u = [\delta_{ti}], \quad w = [R^{-1} \ \dot{R}^{-1} \ \theta_0 \ \dot{\theta}_0 \ \ddot{\theta}_0 \ y_0 \ \dot{y}_0]^T. \tag{4}$$

Note that the state vector $x(t)$ comprises vehicle-related states, the control input vector $u(t)$ is the tilt control command, the exogenous input vector $w(t)$ comprises the set of 'deterministic' components (i.e. linked to curvature and cant) and 'stochastic' components (i.e. linked to lateral track irregularity) of the railtrack. For the definition (and values) of parameters/constants/variables, the reader can refer to Appendix 3. A more rigorous explanation on the state space model is presented in Zolotas et al. (2008) (Table 1).

2.2. Track inputs and performance assessment

The excitation (exogenous) inputs are the low-frequency track disturbance (deterministic track input) and the lateral track irregularities (straight track misalignments in the lateral direction – termed as stochastic track input). In particular, the stochastic track input velocity spectrum is represented by Equation (5) (note v is the vehicle speed (m/s) and f_t is the temporal frequency)

$$\dot{S}_T(f_t) = \frac{(2\pi)^2 \Omega_l v^2}{f_t} \quad (\text{m/s})^2(\text{Hz})^{-1}. \tag{5}$$

Hence, the lateral track velocity represents a coloured noise input and has a steady roll-off as frequency increases. The lateral track roughness used for simulation purposes is $\Omega_l = 0.33 \times 10^{-8}$ m (representing a typically medium-quality rail track). It is worth noting that for ride quality purposes we assess the weighted lateral acceleration of passengers by W_Z Sperling index TF (see Orvnäs, 2011).

The deterministic track (curved track) arises from the intended geometrical layout of the railtrack. This is designed by civil engineers to ensure that the effect upon the passengers meets defined comfort requirements. In particular, for tilting trains the deterministic track relates to (curved sections) track segments with measurable curvature (R^{-1}, R being the curve radius from a virtual inwards curve centre). In addition, the track is leaned inwards or 'canted' in order to rotate the vehicle inwards (hence, minimize the effect of the centrifugal forces experienced by the passengers). Note that the rates of cant and curvature are changing linearly during the curve transitions, while settling on their steady-state values on steady-state curve, see Figure 2.

The misalignment characteristics appear at a higher frequency compared to the deterministic input characteristics. Moreover, the control input is the ideal tilt command (processed via the actuator servo). For more details, the reader is referred to Zolotas and Goodall (2000), Zolotas et al. (2000). For completeness, the track test case information used for simulation and assessment can be seen in Table 2. We note that the (non-tilting) nominal

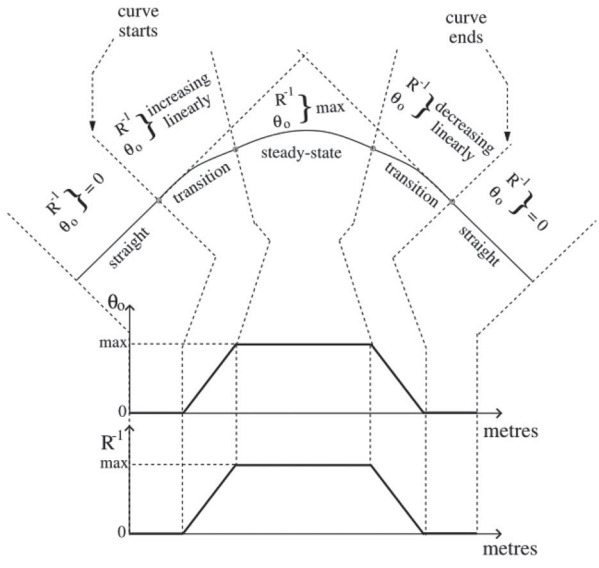

Figure 2. Representation of deterministic track profile.

Table 2. Track profiles used for simulation and assessment (* curved track, † straight track lateral irregularities).

Tilt compensation		60%	Units
Deterministic track*			
Maximum cant angle	$\theta_{o_{(\max)}}$	**6.00**	(degrees)
Maximum curve radius	$R_{\max}$	**1000.00**	(m)
Transition length		145.00	(m) @ each end
Track length		1200.00	(m)
Stochastic track†			
Track roughness	Ω_l	0.33e−8	(m)
Track spatial spectrum	S_T	Ω_l / f^3	$\left(\frac{m^2}{(\text{cycle/m})}\right)$
Track length		1200.00	(m)

vehicle speed is 45 m/s and the (tilting) high speed is 58 m/s.

3. Conventional early nulling-tilt control

Early tilting train control attempted to compensate for the full passenger lateral acceleration on a curved-track. Full compensation (referred to as 'nulling-tilt') was dropped quickly due to high motion sickness by the passengers (Persson et al., 2009; Zolotas & Goodall, 2000). The solution, was to use a portion of the measured acceleration signal and a portion of the vehicle body roll angle (tilt) to provide partial-nulling tilt of 60–70 % compensation of lateral acceleration on steady curve. Figure 3 presents the feedback control concept of the scheme.

The scheme is presented in a typical SISO framework with the design model (nominal-plant) transfer function given by (6). This represents the dynamic relationship between effective cant deficiency $Y_{(e.c.d)}$ (for 60% tilt compensation) and control input $\Delta_{(t-i)}$ (ideal control tilt angle).

$$\frac{y_{e.c.d}}{\Delta_{t-i}}(s) = \frac{27531(s+26.18)}{(s+40.73)\textbf{(s-29.36)(s-6.02)}} \cdots \frac{(s^2+7.65s+24.44)}{(s+23.2)(s^2+1.38s+17.44)(s^2+5.11s+88.02)(s^2+22s+483.6)(s^2+29.15s+4888)(s^2+4.825s+15870)(s^2+41.73s+28440)}. \quad (6)$$

It is worth noting that the effective cant deficiency (the feedback signal) is given by

$$\theta'_{dm} = \left(-\lambda_1 \frac{\ddot{y}_{\text{vm}}}{g} + \lambda_2 \theta_{2sr}\right), \quad (7)$$

where $\ddot{y}_{\text{vm}}$ is the lateral acceleration felt by the passengers as measured from an accelerometer on the body c.o.g (8),

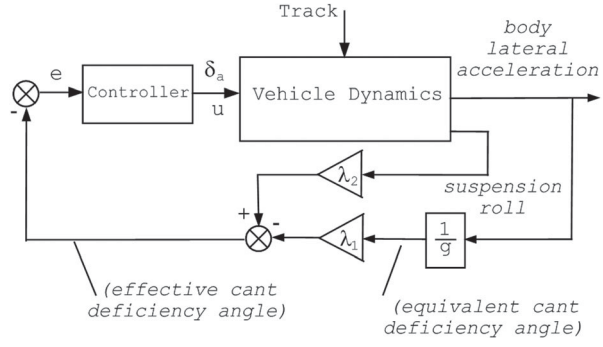

Figure 3. Partial-nulling control feedback setup.

and θ_{2sr} is the secondary suspension roll angle (9).

$$\ddot{y}_{\text{vm}} = \frac{v^2}{R} - g(\theta_o + \theta_{\text{v}}) + \ddot{y}_{\text{v}}, \quad (8)$$

$$\theta_{2sr} = \theta_{\text{v}} - \theta_b. \quad (9)$$

The parameters λ_1, λ_2 are selected to provide 60% tilt compensation on steady curve (typically 0.6, 0.4 respectively, under bogie roll-out angle is neglected). In addition, the classical PID control design nature of the problem studied here does not necessitate model reduction of the plant transfer function.

Previous work in Zolotas and Goodall (2000) presented PI classically tuned control for partial-tilt and the difficulties in achieving stochastic-deterministic tilt performance (which briefly revisited here as basis to enable the reminiscing parts of the proposed enhancement). In addition to the stochastic and deterministic trade-off, the existence of non-minimum phase (NMP) zeros, i.e. zeros in the transfer function of the plant introducing extra phase lag (these are highlighted in Equation (6)) impose performance constraints.

For completeness, we present the pole-zero map of the uncompensated open-loop system in Figure 4, which shows the two zeros on the right hand of the s-plane.[1] The more conservative zero is the slow (closer to the origin from the right). From a speed of system response, the NMP zeros limit the bandwidth of the system which is lower than half of the slower NMP zero frequency (Åström & Hägglund, 2006).

The difficulty with manual design of the controller dealing with the aforementioned plant model was shown previously (Zolotas et al., 2008). Although ride quality degradation for stochastic track can be obtained with a simple (even manually designed) PI controller within the allowed value of 7.5% degradation, satisfying acceptable values of PCT (or P_{CT}) factors (refer to Appendix 2)

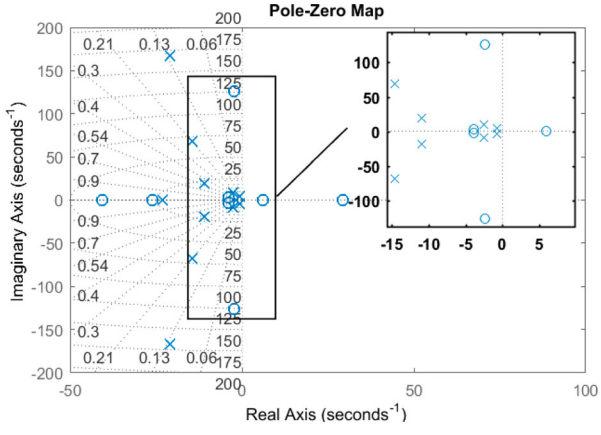

Figure 4. Pole-zero map of the plant transfer function (with zoomed version of nearer-to imaginary axis pole-zero pairs).

for both standing and seating passenger cannot be achieved. In fact, seminal work by Goodall, Zolotas, and Evans (2000) has illustrated that given the industry maximum of around 8–9°, 30% speed-up cannot be achieved without deteriorating the passengers' comfort during curve transitions. Hence, as it is the case in this paper, the PCT factors of the tilting train at higher tilting speed will naturally by higher than the PCT factors at the non-tilting speed.

This paper follows an alternative approach. Firstly, using conventional Z-N PID design and subsequent de-tuning of the controller parameters to improve speed of response. Secondly, designing PID controllers via minimization of different cost functions to addressing the deterministic/stochastic tilt control problem, the optimis4ation in such case is labelled 'tilt-targetted' to distinguish from traditional optimized PID tuning that stems from process-control applications.

4. PID tilt control enhancement via controller optimization

P + I + D (Proportional + Integral + Derivative) controllers are a popular simple classical type of controllers used in a large number of industrial applications (Chen, Yuan, Yuan, Huang, Li, & Li, 2015; Diba, Arora, & Esmailzadeh, 2014; Gopi Krishna Rao, Subramanyam, & Satyaprasad, 2014; Quevedo & Escobet, 2000; Rocco, 1996) including some simple quarter-car suspension systems (Hanafi, 2010; Popovic, Jankovic, & Vasic, 2000; Talib & Darns, 2013). It is of no surprise that it also forms the simplest conventional controller for the tilting active control application, as it offers both the integral action required to force zero effective cant deficiency on steady-curve and the proportional/derivative action to limit phase lag at higher frequencies (compared to the crossover frequency). In this context, conventional P + I and fuzzy P + I + D controllers have been investigated in tilt control previously (Zamzuri et al., 2006b, 2008; Zolotas et al., 2000).

The usual PID controller expression with approximate derivative is employed here, with the derivative cutoff at 1000 rad/s (well above the frequency range of interest for the tilt application).

$$K_{\text{PID}} = k_p\left(1 + \frac{1}{\tau_i s} + \frac{\tau_d s}{\frac{s}{N}+1}\right). \tag{10}$$

The remainder of the parameters is the usual set of: k_p the proportional gain, τ_i the integral time constant and τ_d the derivative time constant. The PID controller is designed to follow tilt control performance requirements on straight and curve tracks. Tilt control systems must maintain a straight track (stochastic) ride quality degradation performance of no more than 7.5% (Förstberg, 2000) while keeping the comfort response of passengers during curve transition (deterministic) in terms of PCT factor as good as non-tilting speed. More explanation on PCT factor can be found in Appendix 2. The trade-off between these two must be achieved. On curved track sections, lateral acceleration perceived by the passengers should be reduced. The full assessment for tilt control can found in Goodall et al. (2000).

4.1. Choice of initial conditions

A natural choice of initial PID gain conditions for the optimization process, especially for the practising control engineer, can stem from the ultimate gain Ziegler–Nichols method, i.e. proportional controller gain: $k_p = 0.6k_u$; integral time constant: $\tau_i = 0.5T_u$, derivative time constant: $\tau_d = 0.125T_u$; whereby k_u is the ultimate gain (i.e. max gain before instability occurs) and T_u is the critical period (i.e. the period of sustained oscillations being the inverse of the crossover frequency. For the case presented in this paper, $k_u = 0.325$ and $T_u = 0.825$s. Therefore, the Z-N (original) PID gains are given as

$$K_{p_{(z-n)}} = 0.195, \quad K_{i_{z-n}} = \frac{K_{p_{(z-n)}}}{\tau_{i_{(z-n)}}} = 0.472,$$

$$K_{d_{z-n}} = \frac{K_{p_{(z-n)}}}{(\tau_{d_{(z-n)}})^{-1}} = 0.02;$$

Ziegler–Nichols is not the only classical tuning rule that can be used Vesely (2003), Tan, Liu, Chen & Marquez (2006), however suffices for the purposes of the work presented here as well as been one of the most popular simplified PID tuning rules. The authors have looked into a number of classical PID tuning rules, amongst other approaches, for the tilt control problem in Hassan, Zolotas, and Margetts (2016).

Undoubtedly different initial condition usually give different tilt assessment results due to the existence of local minima. There are certain ways to prevent the optimization process stuck in local minimum by adding more iterations as well as adding certain bound of controller gain, integral and derivative time constant. We utilize multi-start to perturbing initial conditions in the optimization procedures for completeness (about 10 iterations with a random initial value generation in the interval $[0.01\vec{x}_0, 2\vec{x}_0]$, where $\vec{x}_0$ is a row vector of initial gains given by Z-N rules on the original design model TF). Note that unrealistic gain bounds for the initial conditions would normally result to unrealistic optimization.

We also present results of the de-tuned Z-N PID controller (emphasizing integral action), i.e. Z-N detuned

Table 3. Minimization approach identifiers and constraints (Note: rqd denotes ride quality degradation; GM: gain margin; PM: phase margin).

Minimization ID	f(x)	< constraints >
CF1	ITAE	At least absolute stability
CF2	IAE	At least absolute stability
CF3	ITAE	rqd $\leq 7.5\%$
CF4	ITAE	GM ≥ 1.45, PM $\geq 45^0$
CF5	ITAE	GM ≥ 1.45, PM $\geq 45^0$, rqd $\leq 7.5\%$
CF6	P_{CT} (standing)	GM ≥ 1.45, PM $\geq 45^0$, rqd $\leq 7.5\%$
CF7	P_{CT} (standing)	rqd $\leq 7.5\%$, $\|\|S(j\omega)\|\|_\infty \leq 2$
CF8	P_{CT} (standing)	rqd $\leq 7.5\%$, $\|\|S(j\omega)\|\|_\infty \leq 2$, $\|\|W_\delta(j\omega)T(j\omega)\|\| \leq 1$

Table 4. PID controller designed for the different cost functions.

Design approach	K_{PID} controller TF
Z-N PID (Original)	$\frac{8.377s^2 + 80.57s + 194.7}{0.4129s^2 + 412.9s}$
Z-N PID (De-tuned)	$\frac{4.188s^2 + 40.38s + 194.7}{0.2064s^2 + 206.4s}$
CF1	$\frac{4.254s^2 + 20.56s + 186.3}{0.1093s^2 + 109.3s}$
CF2	$\frac{4.253s^2 + 20.55s + 186.3}{0.1093s^2 + 109.3s}$
CF3	$\frac{5.305s^2 + 43.43s + 243.6}{0.1773s^2 + 177.3s}$
CF4	$\frac{2.468s^2 + 6.957s + 93.67}{0.07328s^2 + 73.28s}$
CF5	$\frac{3.828s^2 + 18.97s + 145.5}{0.1294s^2 + 129.4s}$
CF6	$\frac{2.675s^2 + 8.778s + 92.37}{0.09404s^2 + 94.04s}$
CF7	$\frac{2.098s^2 + 7.161s + 80.63}{0.08781s^2 + 87.81s}$
CF8	$\frac{1.328s^2 + 2.533s + 44.84}{0.05548s^2 + 55.48s}$

gains: $k_p = 0.6k_u$; $\tau_i = 0.25T_u$, $\tau_d = 0.125T_u$; (the original Z-N approach adheres to the 1/4 decay ratio, which does not necessarily incorporate sufficient integral action for the case of the effective cant deficiency). The designed PID controllers for the Z-N approach, as well as the subsequent optimization-based approaches (discussed later in the paper) can be seen in Table 4. Moreover, Table 5 presents the tilt performance results of the Z-N controller designs (Figure 5).

4.2. PID tuning via time-domain cost function optimization

There are four typical and widely popular performance indices for PID design in the time domain widely used in the PID control literature, and a natural set of metrics in process control applications (Ho, Lim, & Xu, 1998; Panagopoulos, Åström, & Hägglund, 2002). Namely the ISE (integral of squared error), IAE (integral of absolute error), ITSE (integral of time multiply squared error) and ITAE (Integral time of absolute error). Other ways of setting up PID controller design via global optimization with generic additional constraints can be seen in Ozana and Stepan (2016). In this paper we focus on IAE and ITAE, since these are the ones used more frequently in PID tuning (Ho et al., 1998; Zamzuri et al., 2006b). We follow the usual formulae for ITAE and IAE costs:

$$J_{(\text{itae})} = \int_0^\infty t|e(t)|\,\mathrm{d}t, \tag{11}$$

$$J_{(\text{iae})} = \int_0^\infty |e(t)|\,\mathrm{d}t, \tag{12}$$

respectively, where $e(t)$ represents an error signal in the feedback control framework, i.e. minimization of a form of error in the closed-loop system. For the tilt control application is the effective cant deficiency, i.e. the signal that establishes partial-tilt compensation on curved track.The ITAE and IAE cost functions are set up in the usual constrained optimization approach given by

$$\begin{aligned} &\underset{K_{\text{pid}}}{\text{minimize}} \quad f(x) \\ &\text{subject to} \quad \textbf{constraints} \end{aligned} \tag{13}$$

For the tilt application, a number of constraints are included and given in Table 3. The different constraints emphasize the increasingly stringent tilt performance speed.

The above minimization procedure can be setup in a straightforward manner in one of the currently available software tools. In this paper Matlab was employed via use of function *fmincon* (an alternative approach is via use of *fminsearch* with appropriate constraints). Few remarks: (i) in CF1 and CF2 'at least absolute stability' essentially constrained by a least bound of (gain margin) GM $= 1.2$, and (phase margin) PM $= 20$ deg., (ii) CF8 introduces a bound on multiplicative uncertainty to guarantee robust stability (details on this will be shown in later sections), (iii) We opt to using minimization of PCT (standing) as this forms the worst-case PCT factor metric.

It is worth noting that the allowed GM and PM bounds represent a typical set of accepted design margins for railway vehicle suspensions, i.e. a gain margin of not less than 3dB and a phase margin of not less than 45°. The bound for the peak of the sensitivity function $S(j\omega)$ attempts to maintain a level of allowed worst-case performance degradation (values of less than 2 (6 dB) can be tried but will impose a hard design constraint for the tilt control application given in the nmp zeros. A value of 2 (6 dB) is still acceptable to provide a minimum level of damping also see Skogestad & Postlethwaite, 2007). Similarly the one for the peak of the robust stability $W_\delta(j\omega)T(j\omega)$ function is imposed by robust control theory

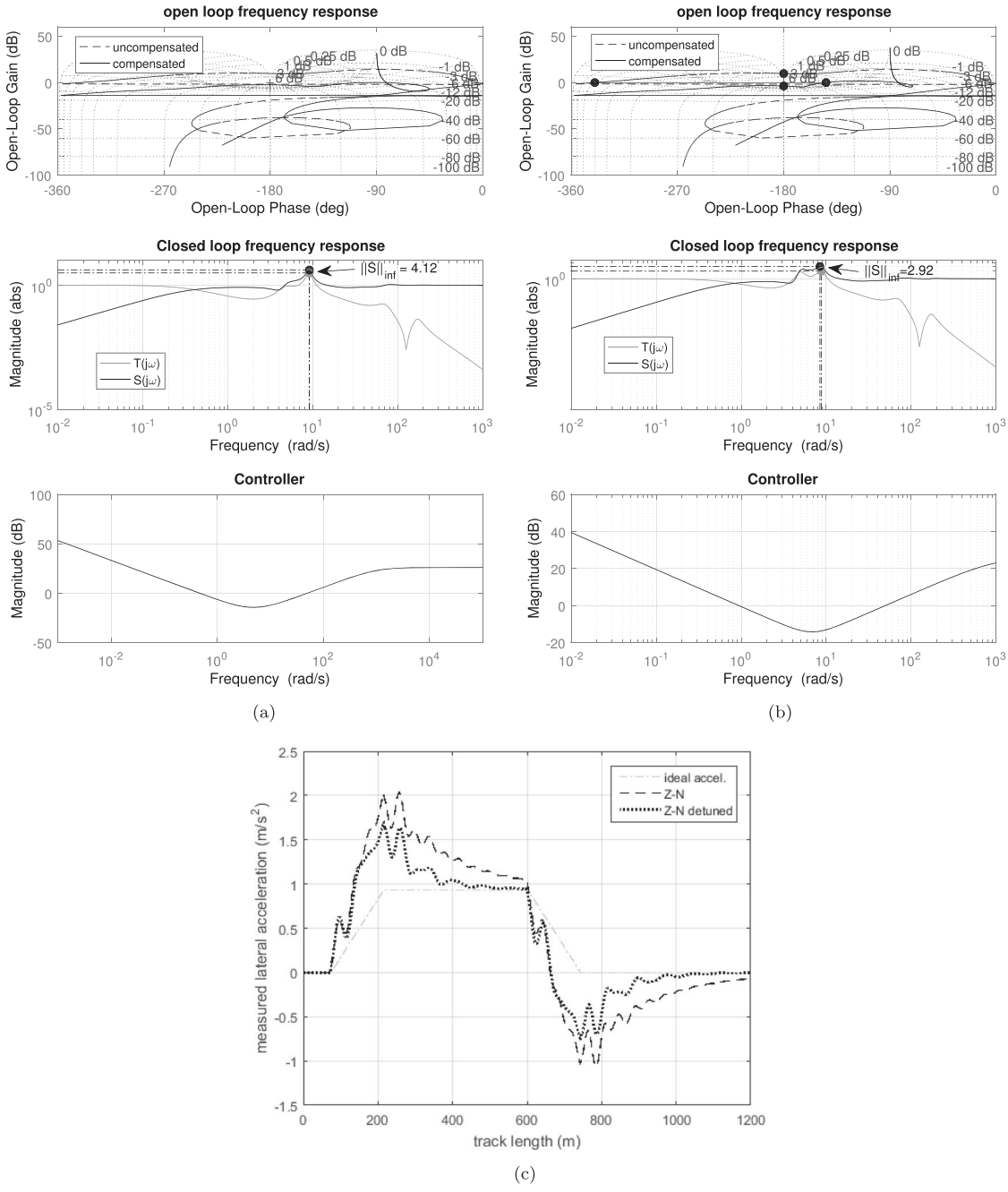

Figure 5. Magnitude frequency responses for the two PID Z-N cases and their deterministic lateral accel. response. (a) PID controller via Z-N, (b) PID controller via Z-N detuned and (c) Lateral acceleration deterministic.

(essentially driven by choice of W_δ) (Skogestad & Postlethwaite, 2007). The choice of weighting function W_δ in this work characterizes the model uncertainty for the tilt vehicle model.

The tilt performance results via different optimizations and constraint identifiers are shown in Table 5, and discussed further in the section of results and discussion. For completeness the designed PID controllers for the different cost functions can be seen in Table 4.

5. Results and discussion

The following sections begin by analysing the results on the nominal system, then extends discussion to performance under parametric perturbations from a robustness point of view of the proposed controller solutions.

A few remarks noted here: (i) the designed PID controllers are not directly compared to other non-PID-based design tilt control methodologies as the purpose of

Table 5. PID controller performance assessment with the different time-domain optimization approaches.

	Deterministic(as per given units)	Z-N PID original	Z-N PID detuned	CF1	CF2	CF3	CF4	CF5	CF6	CF7	CF8
Lateral accel.	RMS Deviation (%*g*)	6.22	4.066	2.775	2.775	3.291	3.325	3.612	3.997	4.204	4.625
	Peak value (%*g*)	20.797	17.348	15.370	15.367	16.199	15.081	16.290	16.660	16.979	17.749
Roll gyro.	RMS deviation (rad/s)	0.034	0.029	0.027	0.027	0.031	0.026	0.027	0.028	0.029	0.031
	Peak value (rad/s)	0.079	0.091	0.119	0.119	0.108	0.099	0.099	0.090	0.090	0.088
P_{CT} related	Peak jerk level (%g/s)	11.499	9.703	9.857	9.857	9.824	8.962	9.603	9.313	9.307	9.280
	Standing (% of passenger)	76.192	65.153	66.833	66.829	66.141	58.98	63.68	62.3	63.1	64.834
	Seated (% of passenger)	24.698	20.339	19.724	19.722	20.025	17.895	19.570	19.342	19.604	20.198
	Stochastic (acceleration %g) @58 m/s**										
	**Ride quality for non-tilting train if running at the higherspeed = 2.848 %g										
Ride quality	Tilting train	2.709	2.936	3.642	3.642	3.062	3.373	3.062	3.062	3.061	3.031
	Degradation (%)	−4.884	3.1	27.873	27.88	7.5	18.448	7.5	7.5	7.49	6.412

this paper is to rigorously investigate the achieved PID performance for the partial-nulling-tilt control problem (the interested reader can refer to the cited tilt papers, throughout this manuscript, and references within) to note the usefulness of more advanced control design methods compared to PID); (ii) an optimized PID tilt controller (as seen in this work) can potentially be employed as baseline filter/shaper for more advanced control approaches in tilt control-related problems; (iii) the SISO tilt TF is used for design purposes, while results run on simulink with the full-order (excited by all exogenous inputs) end-view tilt model.

5.1. Nominal performance (nominal plant and designed controllers)

With reference to results from Table 4 on the use of minimization of the conventional ITAE (CF1) and IAE (CF2) (with at least absolute stability) these offer improvement in deterministic tilt performance (i.e. see Table 5) but largely degraded ride quality (stochastic). The aforementioned kind of minimization does provide controllers that drive the system closer to instability (being optimization on time-domain signal), hence the results are not surprising. The performance indices above could be used as a starting point for the PID design, but offer no advantage in the overall tilt performance.

CF3 minimizes ITAE while constraining ride quality to being up to 7.5% degraded. The minimization process provides controller values that attempt to address the trade-off (the ITAE being related to the deterministic side, while the ride quality constraining the allowed stochastic side degradation). The CF3 results show that increasing the PM improves damping, which gives improved ride quality performance and deterministic improvement due to the reduced peak value of the roll gyroscope signal.

The overall situation is largely improved once more direct stability margin constraints are included, i.e. GM and PM bounds to achieve. We then note the amount of module margin (i.e. the H-infinity norm of the designed system sensitivity transfer function) the proposed minimization process provides (as with only a PID controller it is rather challenging to constrain the sensitivity peak for the tilt control design without substantially affecting speed of response) (Table 6).

Table 6. Stability margins for the controllers(GM, gain margin: PM, phase margin).

Design approach	GM(dB)	PM(deg)	CL B/W (rad/s)	$\|\|S(j\omega)\|\|_\infty$
Z-N PID original	2.40	80.9	0.486	4.12
Z-N PID de-tuned	3.7	35	0.98	2.92
CF1	1.45	15.0	3.95	6.16
CF2	1.42	10.0	4.16	7.7
CF3	1.44	21.9	4.15	6.68
CF4	3.22	44.9	1.2	3.22
CF5	3.23	45.1	1.12	3.23
CF6	4.1	91.8	0.9	2.63
CF7	6	91.45	0.84	2
CF8	6.01	89.9	0.71	1.99

Figure 6 presents the bode plot for the designed PID controllers, whereby small differences may be seen however this supports that refined tuning does have a substantial impact on the tilt performance. Moreover, Figure 7(c) and 7(d) presents frequency and time-domain results for CF3, CF4 and CF5. The slower response due to the improved stability margins is evident (compared to Figure 7(a) and 7(b) for CF1 and CF2). The lateral acceleration response is improved for CF6, CF7 and CF8 cases with larger phase margin (Figure7(e) and 7(f)). In the compensated open-loop figures, the cumbersome nature of finely shaping the module margin with only a PID controller is shown.

For completeness, Figure 8 presents the sensitivity of the system (nominal plant and listed controllers in the figure) to the stochastic track input disturbance (rate of lateral track irregularity to filtered lateral acceleration for passenger comfort). The noted region on the figure indicates changes that have an impact on the ride quality value. Recall that active tilt will tend to degrade the ride quality (thus, the industrially accepted bound of 7.5% worst as discussed previously) (Goodall et al., 2000). We

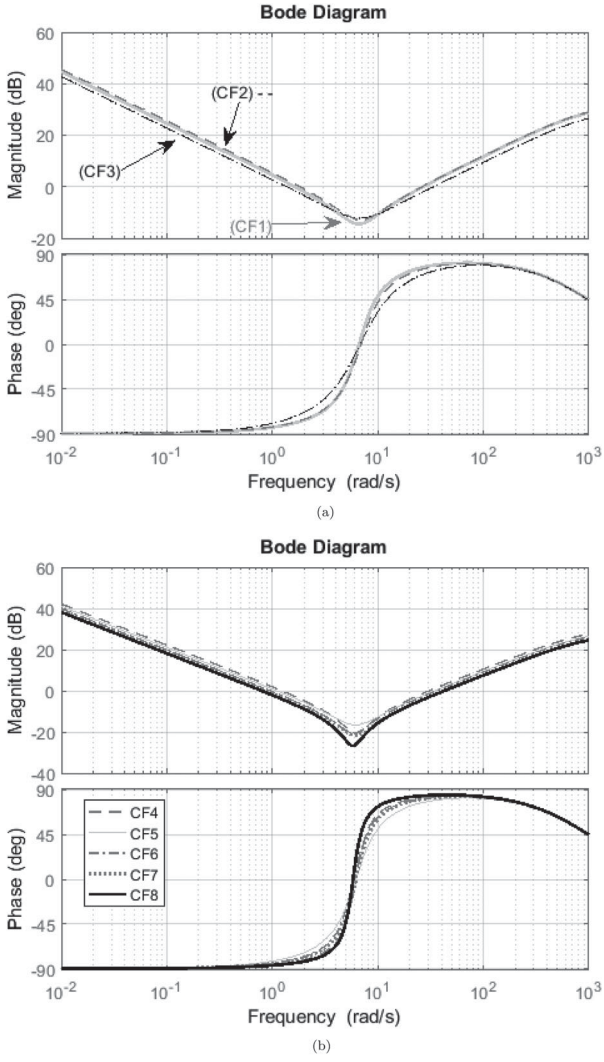

Figure 6. PID controllers bode plot. (a) CF1, CF2, CF3 and (b) CF4-8.

also present the result on sensitivity to matched uncertainty (see Figure 9).

5.2. Robustness analysis

In this section we briefly discuss fundamental robust performance considerations for the proposed designs. The analysis is twofold, (i) four perturbed plant models are considered (alongside the nominal model the controllers were designed on) using the nominal controllers, and (ii) controller uncertainty is considered using the nominal model (i.e. a basic form of controller fragility investigation).

5.2.1. Case (i) Plant perturbations and nominal controllers.

For case (i) the nominal plant model case is referred to as P0, and the perturbed plant model cases as P1, P2, P3 and P4, respectively. Table 7 presents the details on model perturbations considered in the work. We note the following in terms of the perturbation cases: the variation of vehicle body mass serves as a mechanism to affect (vehicle dynamics) but in particular non-minimum phase zero (NMPZ) locations, while the variation of the listed secondary suspension parameters will affect vehicle dynamics (but not the NMPZ locations). This offers a wider level of assessing performance under uncertainty (rather than just addressing only non-minimum phase location uncertainty). It is also worth noting that cases P3 and P4 are seen as challenging ones for the rail application (at such levels the vehicle will undergo maintenance, however, we consider it at a theoretical level for robustness analysis). The addressed plant uncertainty can be also translated into multiplicative uncertainty form (Skogestad & Postlethwaite, 2007), i.e.

$$G_p(j\omega) = G_{nom}(j\omega)(1 + W_\delta(j\omega)\Delta(j\omega)) \quad \text{with } \Delta(j\omega) \text{ stable and } \|\Delta(j\omega)\|_\infty \leq 1 \tag{14}$$

(see Figure 10) with an identified fourth-order bound $W_\delta(j\omega)$ below

$$W_\delta(s) = \frac{0.5481s^4 + 10.31s^3 + 143.7s^2 + 228s + 186.3}{s^4 + 9.505s^3 + 240.8s^2 + 454.3s + 2555} \tag{15}$$

Although a higher order multiplicative uncertainty bound $W_\delta(j\omega)$ can be identified, the above order is sufficient for the analysis in the paper. The magnitude plot for the multiplicative uncertainty and the identified bound $W_\delta(j\omega)$ is shown in Figure 10. Note that this form of bound was included in the constrained optimization CF8.

Figure 11 presents the bode plot of the nominal plant (uncompensated open-loop) together with all perturbed plant cases (the change of the uncompensated Open-Loop (OL) stability margins is clearly seen). Figure 12 shows the sensitivity magnitude plot for CF4,CF5,CF6,CF7 and CF8, respectively. The three different cases (CF4,CF5 and CF6) have very similar frequency response characteristics. Still, a peak value between 7 and 8 dB indicates some robustness considerations (Skogestad & Postlethwaite, 2007). The sensitivity peak of 2(6 dB) can be achieved for CF7 and CF8 as expected (see Table 3). In addition for CF8, the complimentary sensitivity ($T(j\omega)$) is constrained to be below the multiplicative uncertainty ($W_\delta(j\omega)$) bound hence guaranteeing the required robust stability (see Figure 13).

Since PID controller case CF4 fails to maintain acceptable rqd and infact cases CF4, CF5 and CF6 present similar frequency response characteristics, only PID controller CF6 is considered for the robustness analysis. Thus CF6 PID controller is compared to the conventional Z-N

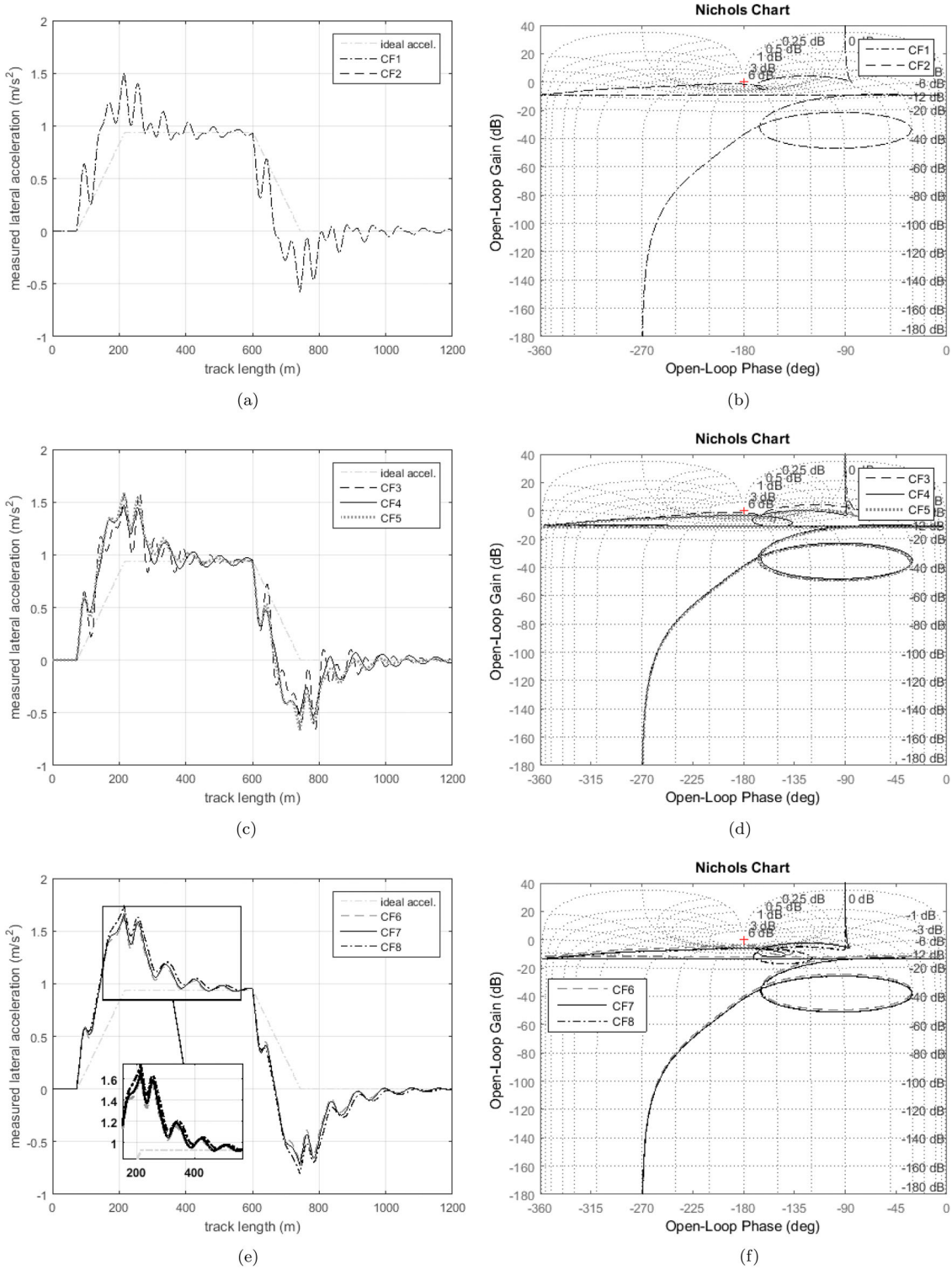

Figure 7. Deterministic lateral acceleration and Nichols plot of designed $L(j\omega)$ results for the different PID controllers. (a) Lateral acceleration, (b) Compensated open-loop freq. resp., (c) Lateral acceleration, (d) Compensated open-loop freq. resp., (e) Lateral acceleration and (f) Compensated open-loop freq. resp.

detuned case, CF3, CF7 and CF8 so as to illustrate the different controller class performance.

Tables 8 and 9 present results for ride quality and PCT factor for the perturbed cases alongside the nominal case. Figure 14 presents the compensated OL frequency response for all above cases. It is clearly seen that as Z-N detuned and CF3 controllers drive the system to instability in a couple of cases (note the nature of ITAE minimization is to provide designs closer to instability) but mostly give small PCT factor values in other cases.

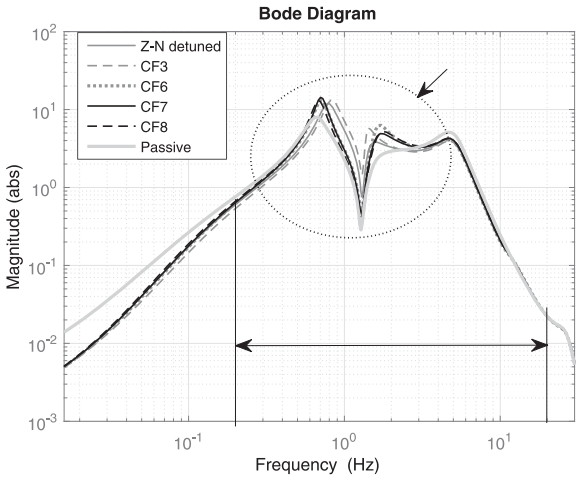

Figure 8. Ride quality TF for different controllers and nominal plant.

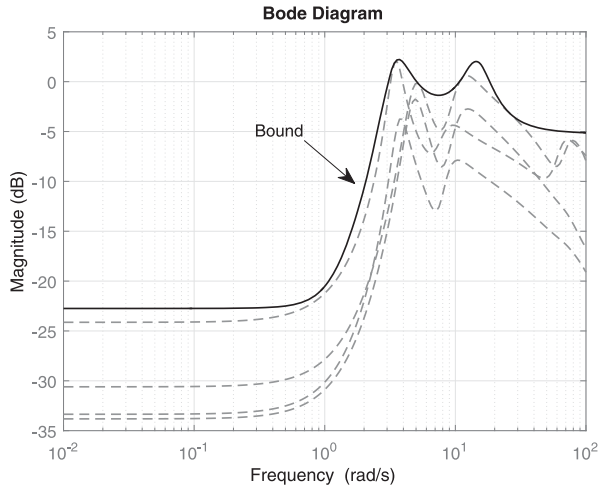

Figure 10. Multiplicative uncertainty and bound ($W_\delta(j\omega)$, fourth-order TF).

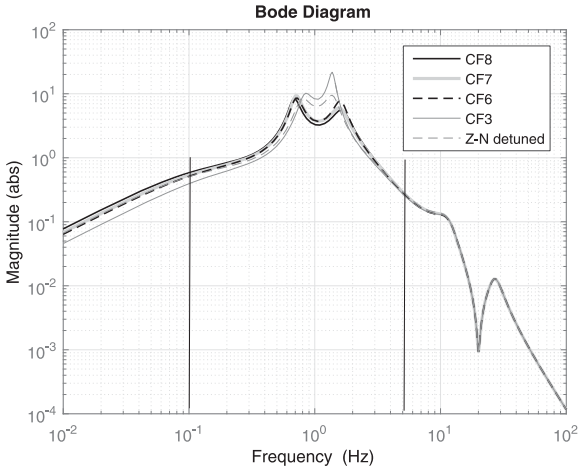

Figure 9. Sensitivity to Input (disturbance), i.e. Matched uncertainty, (for the different controllers).

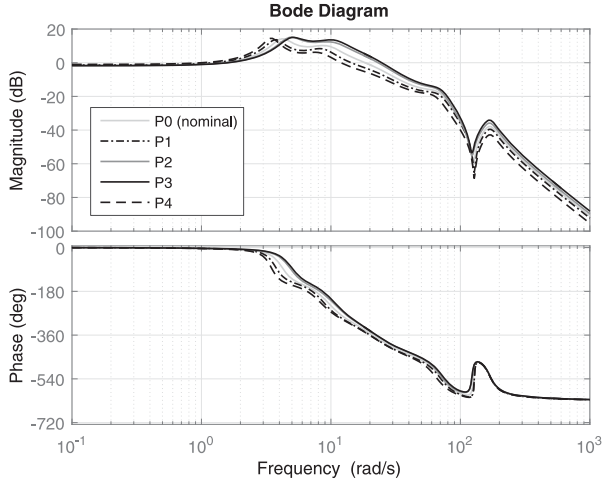

Figure 11. Bode plot of nominal and perturbed plants.

Table 7. Perturbed plant cases.

Plant ID	Perturbation
P1	20% body mass increase
P2	20% body mass decrease
P3	20% decrease in dynamic body mass and 40% (20%) decrease (increase) in secondary suspension damping (stiffness)
P4	20% increase in dynamic body mass and 30% (20%) decrease (increase) in secondary suspension stiffness (damping)

CF6 controller is a more robustified case hence manages to perform better than the previous two controllers in almost all uncertainty cases. CF7 and naturally CF8 controllers overall outperform the other controllers in terms of robust stability. No instability occurs for the perturbations while maintaining realistically small values for PCT. Note that the ride quality criterion was not directly considered in terms of robust performance and in this context

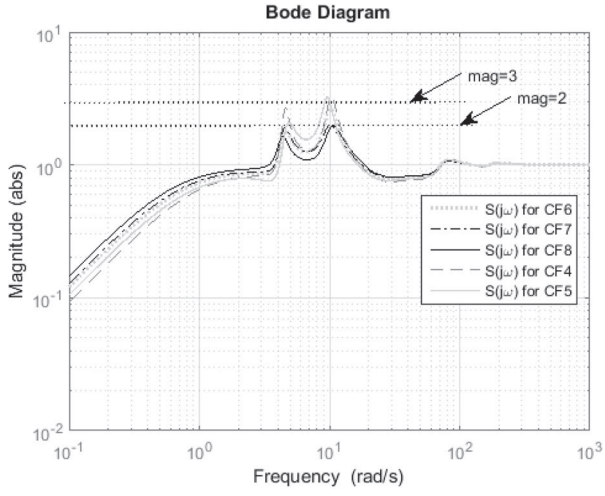

Figure 12. Sensitivity peak of CF4, CF5, CF6, CF7 and CF8.

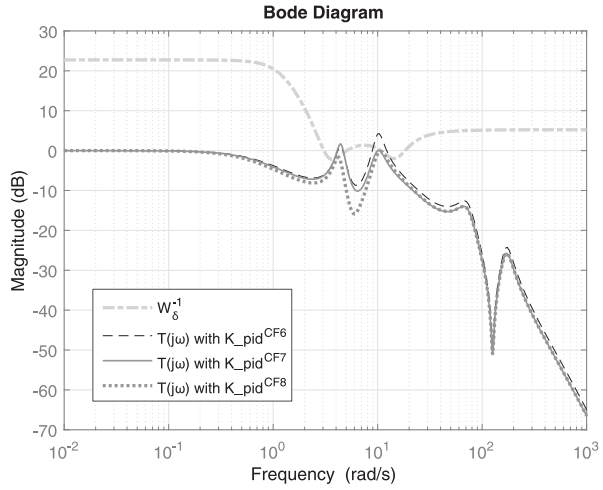

Figure 13. Complimentary sensitivity with multiplicative uncertainity bound.

Table 8. Ride quality performance for designed closed loop (robustness to perturbation); unit is %g.

Plant ID	Z-N Detuned	CF3	CF6	CF7	CF8
P0	3.1	7.5	7.5	7.49	6.41
P1	9.95	20.55	13.66	15.45	11.61
P2	−1.33	Unstable	50.97	9.07	12.10
P3	Unstable	Unstable	Unstable	33.65	40.83
P4	27.87	135.56	36.36	40.35	24.96

Table 9. P_{CT} standing performance for designed closed loop (robustness to perturbation); unit is % of passengers.

Plant ID	Z-N Detuned	CF3	CF6	CF7	CF8
P0	65.15	66.14	62.3	63.1	64.83
P1	63.2	59.21	62.57	63.68	66.1
P2	81.32	Unstable	68.68	65.01	66
P3	Unstable	Unstable	Unstable	69.54	67.47
P4	64.81	62.86	65.56	67.11	70.12

the controllers with plant cases P3 and P4 – not surprisingly – fail to maintain the ride quality performance.

The above discussion supports the findings in the previous section, i.e. that the sensitivity plot's peak values indicated some robust performance concerns. This is not surprising as still a simple PID controller is used and, via the proposed design, the extent to which it handles the tilt control performance issues in the presented framework is shown (noting that the objective of the paper is to re-visit simple PID control and rigorously investigate its capabilities for tilt control).

Through close look on the controllers for the robustness considerations in this section, the decision on the 'better' PID controller design case, to either use as is or employ as a baseline filter for further advanced control design considerations, leans towards CF7 and CF8. These PID controller version attempt to maintain a rather consistent set of deterministic (and in some cases stochastic) results under uncertainty (with some conservativeness in some cases). Actually, from a strict theoretical robust stability point of view CF8 can be labelled as the primary choice.

5.2.2. *Case (ii) Nominal plant and controller uncertainty.*

Regarding case (ii) no plant perturbation is utilized while the controller uncertainty considered for the analysis is given in Table 10. Controller uncertainty (or fragility) may arise from discrepancies in the controller implementation or minor faults in the controller algorithm/structure (software or hardware). The controller perturbations are referred to as CP1, CP2, CP3 and CP4. Note that controller uncertainty will have a slightly different pattern of performance impact compared to the plant perturbations (seen in the previous section).

Note that controller CF3 is a controller which suffers from providing good robustness properties to the designed closed-loop system (as seen previously) and we do not consider it here. However, we refer to controllers Z-N detuned, CF6, CF7, CF8 to illustrate performance changes given the aforementioned controller uncertainty (fragility). Figure 15 presents a set of deterministic/stochastic trade-off characteristics (the *x*-axis is common and refers to the ride quality degradation (stochastic) while the left and right *y*-axis refer to the deterministic criterion i.e. P_{CT} factor (standing) and max passenger acceleration respectively). The (mostly) Pareto trend in the trade-off is still seen, with CF6 and CF7 tending to provide the better performance compared to the Z-N (detuned) PID version while CF8 provides slightly more conservative result compared to CF6 and CF7. Still taking in account both performance against plant uncertainty and performance against controller fragility, it is controller CF8 that mostly stands out (with CF7 the close second choice). Note that essentially controller CF8 is an enhanced version of CF7 (as it adheres to the design using the same cost function and constraints with the addition of the multiplicative uncertainty bound).

Note that in either case of deterministic criterion (left or right *y*-axis) one can see the similar trend relative to the stochastic criterion (hence only one deterministic criterion could be utilized for analysis purposes if necessary). It is worth noting that while it may – visually – seem controller perturbation providing better trade-off results, it is the nominal controller that ultimately provides the desired levels of deterministic/stochastic trade-off result as discussed in the previous sections.

6. Conclusion

This paper revisits simple PID controller design for the problem of railway active tilt control suspensions and

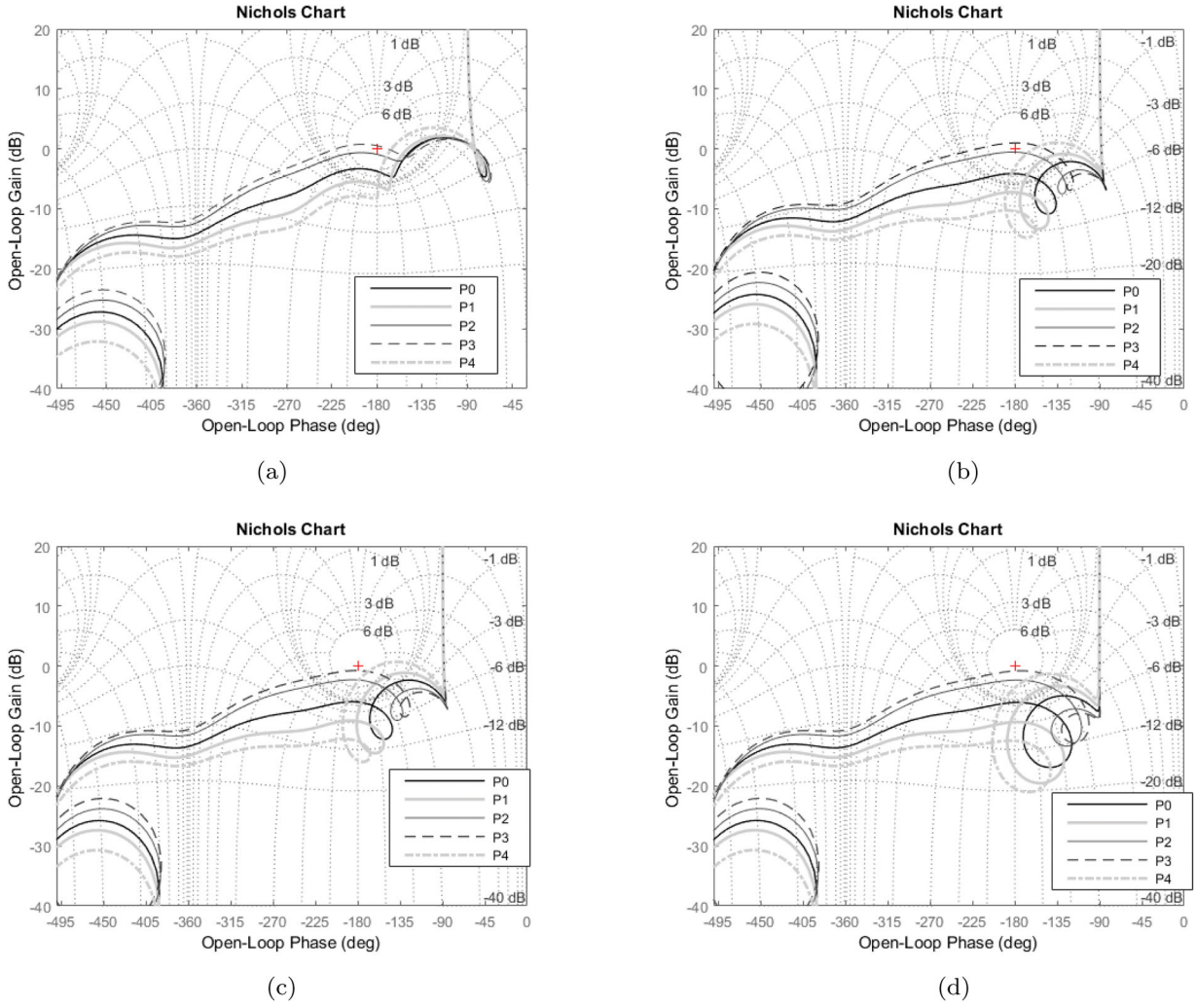

Figure 14. Robustness assessment of compensated OL frequency responses. (a) Z-N detuned, (b) CF6, (c) CF7 and (d) CF8.

Table 10. Controller uncertainty cases.

Controller ID	Perturbation
CP1	20% increase gain k_p, 20% decrease integral gain τ_i, 20% increase derivative gain τ_d
CP2	20% decrease gain k_p, 20% increase τ_i, 20% decrease τ_d
CP3	20% increase gain k_p
CP4	20% decrease gain k_p

presents a rigorous study on enhanced PID tilt control design via optimization. The problem was posed in a straightforward single-input–single-output control framework. Using constrained optimization we appraise and compare different PID controller designs for the deterministic (curved track) and stochastic (track irregularities) trade-off, within the per-vehicle tilt control non-minimum phase zero limit (essentially recommended levels of achievement using optimized conventional PID). The advantage of additional constraints in the cost functions esp. on stability margins and robustness bounds is shown. Detailed performance results for the nominal models as well as discussion of robustness (to both plant uncertainty and controller fragility) is presented, including suggestions for which of the approaches could be employed as a baseline for further considerations. With no loss of generality, the PID control design suggestions in the paper can be followed for active suspensions of similar nature. Undoubtedly other combinations of cost function and constraints could be pursued (it is the nature of optimized PID design that allows for a plethora of approaches). However, the ones presented here refer to a series of SISO tilt control targeted concerns that offer a decision support tool for the practising control engineer. Current work of the authors relates to enhancement of robust performance of further tilt control solutions and implementation on rail vehicle simulation software.

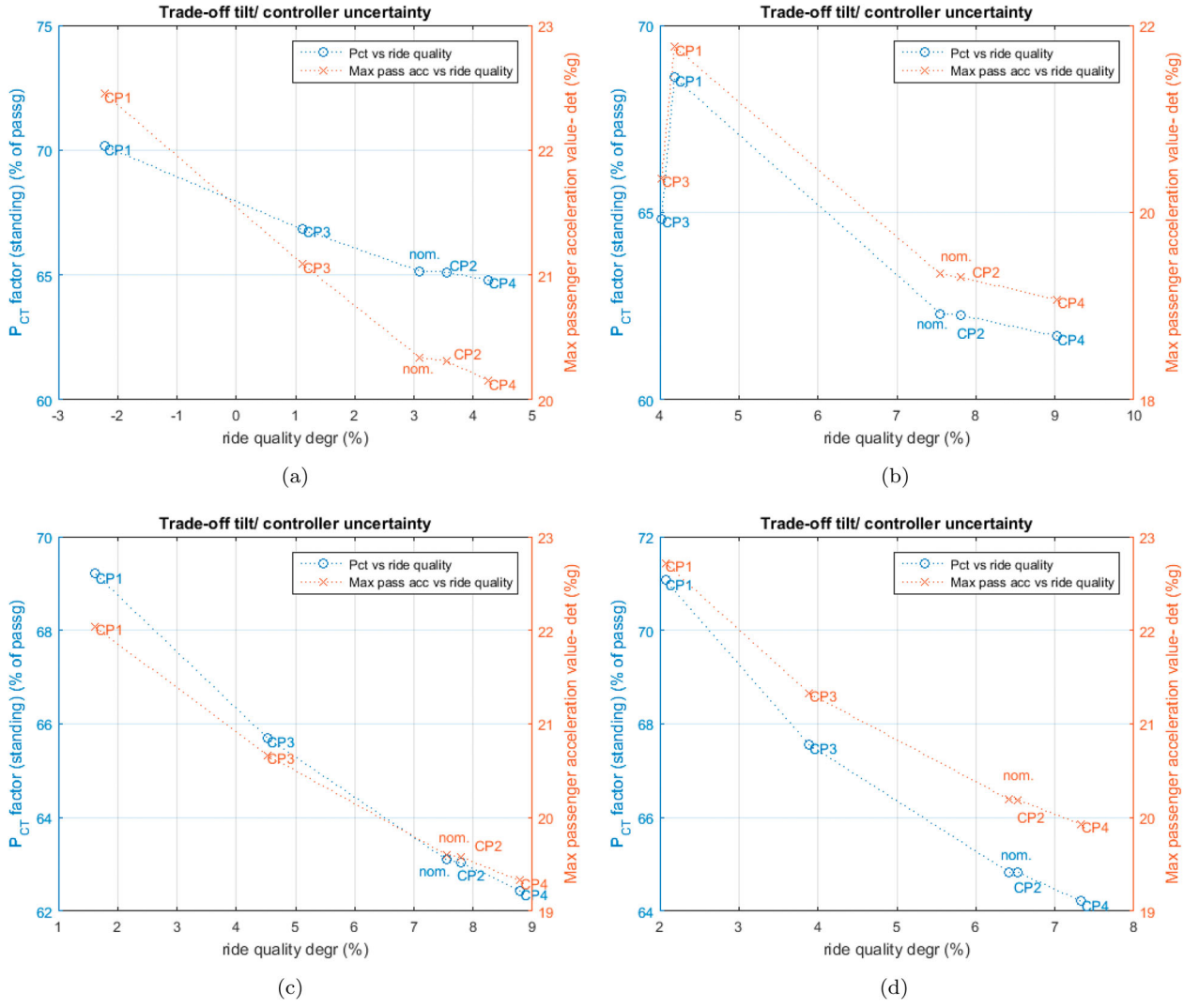

Figure 15. Deterministic-Stochastic trade-off investigation on controller uncertainty with nominal plant: P_{CT} factor (standing) vs. ride quality degr., and peak passg accel. vs. ride quality degr. (a) Z-N Detuned, (b) CF6, (c) CF7 and (d) CF8.

Note

1. For zooming within matlab-produced figures, we have used On-Figure magnifier (http://uk.mathworks.com/matlabcentral/fileexchange/26007-on-figure-magnifier)

Acknowledgments

The authors acknowledge computer facilities support from the School of Engineering, University of Lincoln. The authors would also like to thank the anonymous reviewers for their constructive comments, which helped us to further improve the quality of this manuscript. The first author acknowledges Majlis Amanah Rakyat (MARA) Malaysia for supporting the doctoral studies under PhD scholarship ref. 330407137000.

Disclosure statement

No potential conflict of interest was reported by the authors.

ORCID

F. Hassan http://orcid.org/0000-0003-2992-7355
A. C. Zolotas http://orcid.org/0000-0002-2829-1298
R. M. Margetts http://orcid.org/0000-0003-2990-5316

References

Åström, K. J., & Hägglund, T. (2006). *Advanced PID Control*. Research Triangle Park, NC: ISA – The Instrumentation, Systems, and Automation Society.

Bruni, S., Goodall, R., Mei, T. X., & Tsunashima, H. (2007). Control and monitoring for railway vehicle dynamics. *Vehicle System Dynamics*, *45*(7-8), 743–779.

Chen, Z., Yuan, Y., Yuan, X., Huang, Y., Li, X., & Li, W. (2015). Application of multi-objective controller to optimal tuning of PID gains for a hydraulic turbine regulating system using adaptive grid particle swam optimization. *ISA Transactions*, *56*, 173–187.

Colombo, E. F., Di Gialleonardo, E., Facchinetti, A., & Bruni, S. (2014). Active carbody roll control in railway vehicles using hydraulic actuation. *Control Engineering Practice*, *31*, 24–34.

Diba, F., Arora, A., & Esmailzadeh, E. (2014). Optimized robust cruise control system for an electric vehicle. *Systems Science and Control Engineering*, *2*(1), 175–182.

Förstberg, J. (2000). *Ride comfort and motion sickness in tilting trains* (TRITA-FKT report 2000:28). Stockholm: KTH Railway Technology.

Fröidh, O. (2008). Perspectives for a future high-speed train in the Swedish domestic travel market. *Journal of Transport Geography*, *16*(4), 268–277.

Goodall, R. M., Zolotas, A. C., & Evans, J. (2000). *Assessment of the performance of tilt system controllers*. Proceedings of the railway technology conference IMechE (No. C580/028), Birmingham, UK (pp. 231–239).

Gopi Krishna Rao, P. V., Subramanyam, M. V., & Satyaprasad, K. (2014). Design of internal model control-proportional integral derivative controller with improved filter for disturbance rejection. *Systems Science and Control Engineering*, *2*(1), 583–592.

Hanafi, D. (2010). PID controller design for semi-active car suspension based on model from intelligent system identification. In *Proceedings of the 2nd international conference on computer engineering and applications* (pp. 60–63). IEEE.

Hassan, F., Zolotas, A., & Margetts, R. (2016). Improved PID control for tilting trains. In *2016 IEEE international conference for students on applied engineering (ICSAE)*. IEEE, October, 2016 (presented to appear on IEEE Xplore).

Ho, W. K., Lim, K. W., & Xu, W. (1998). Optimal gain and phase margin tuning for PID controllers. *Automatica*, *34*(8), 1009–1014.

Huber, B. H. (1998). The bogie-based tilt option-simplicity and flexibility. *Proceedings of the Institution of Mechanical Engineers, Part F: Journal of Rail and Rapid Transit*, *212*(1), 19–32.

Iwnicki, S. (Ed.) (2006). *Handbook of railway vehicle dynamics CRC Press*. Boca Raton, FL: Taylor and Francis Group.

Orvnäs, A. (2009). Active lateral secondary suspension in a high-speed train to improve ride comfort. (Master Thesis). KTH, Stockholm.

Orvnäs, A. (2011). *On active secondary suspension in rail vehicles to improve ride comfort* (Doctoral thesis). KTH, Sweden.

Ozana, S., & Docekal, T. (2016). PID controller design based on global optimization technique with additional constraints. *Journal of Electrical Engineering*, *67*(3), 160–168.

Panagopoulos, H., Åström, K. J., & Hägglund, T . J. (2002). Design of PID controllers based on constrained optimisation. *IEEE Proceedings-Control Theory and Applications*, *149*(1), 32–40.

Pearson, J. T., Goodall, R. M., & Pratt, I. (1998). Control system studies of an active anti-roll bar tilt system for railway vehicles. *Proceedings of the Institution of Mechanical Engineers, Part F: Journal of Rail and Rapid Transit*, *212*(1), 43–60.

Persson, R., Goodall, R. M., & Sasaki, K. (2009). Carbody tilting–technologies and benefits. *Vehicle System Dynamics*, *47*(8), 949–981.

Popovic, V., Jankovic, D., & Vasic, B. (2000). *Design and simulation of active suspension system by using Matlab*. Proceedings of FISITA world automotive congress, Seoul, S. Korea.

Quevedo, J., & Escobet, T. (2000). *Digital control: Past, present and future of PID control*. Elsevier Science Inc.

Rocco, P. (1996). Stability of PID control for industrial robot arms. *IEEE Transactions on Robotics and Automation*, *12*(4), 606–614.

Shinmura, H., Hayashi, T., Okada, N., & Kamikawa, N. (2015). Railway vehicle body tilting system. *US Patent 9,090,267*, July.

Skogestad, S., & Postlethwaite, I. (2007). *Multivariable feedback control analysis and design*. New York: Wiley.

Stribersky, A., Steidl, S., Müller, H., & Rath, B. (1996). On dynamic analyses of rail vehicles with electronically controlled suspensions. *Vehicle System Dynamics*, *25*(S1), 614–628.

Talib, M. H. A., & Darns, I. Z. M. (2013). *Self-tuning PID controller for active suspension system with hydraulic actuator*. In Computers and informatics (ISCI), 2013 IEEE symposium (pp. 86–91).

Tan, W., Liu, J., Chen, T., & Marquez, H. J. (2006). Comparison of some well-known PID tuning formulas. *Computers and Chemical Engineering*, *30*(9), 1416–1423.

Veselý, V. (2003). Easy tuning of pid controller. *Journal of Electrical Engineering*, *54*(5-6), 136–139.

Vickerman, R. (1997). High-speed rail in Europe: Experience and issues for future development. *The Annals of Regional Science*, *31*(1), 21–38.

Zamzuri, H., Zolotas, A. C., & Goodall, R. M. (2006a). Intelligent control approaches for tilting railway vehicles. *Vehicle System Dynamics*, *44*(sup1), 834–842.

Zamzuri, H., Zolotas, A. C., & Goodall, R. M. (2006b, September 30–October 1). *Optimised intelligent tilt controller scheme using genetic algorithms*. UKACC International control conference, Glasgow, UK.

Zamzuri, H., Zolotas, A. C., & Goodall, R. M. (2008). Tilt control design for high-speed trains: A study on multi-objective tuning approaches. *Vehicle System Dynamics*, *46*(S1), 535–547.

Zhou, R., Zolotas, A., & Goodall, R. (2010). *LQG control for the integrated tilt and active lateral secondary suspension in high speed railway vehicles*. Control and automation (ICCA). Paper presented at the 8th IEEE international conference, Xiamen, China (pp. 16–21).

Zhou, R., Zolotas, A., & Goodall, R. (2013). *H-infinity based control system and its digital implementation for the integrated tilt with active lateral secondary suspensions in high speed trains*. Paper presented at the 32nd Chinese control conference (CCC) (pp. 5554–5559).

Zhou, R., Zolotas, A., & Goodall, R. (2014). Robust system state estimation for active suspension control in high-speed tilting trains. *Vehicle System Dynamics*, *52*(sup1), 355–369.

Zolotas, A. C., & Goodall, R. M. (2000). *Advanced control strategies for tilting railway vehicles*. UKACC international conference on control, University of Cambridge, Cambridge, UK. 6p., ISBN: 0-85296-240-1.

Zolotas, A. C., Goodall, R. M., & Halikias, G. D. (2002). New control strategies for tilting trains. *Vehicle System Dynamics*, *37*(sup1), 171–182.

Zolotas, A. C., Halikias, G. D., & Goodall, R. M. (2000). *A comparison of tilt control approaches for high speed railway vehicles*. In Proceedings ICSE, Coventry, UK (pp. 632–636).

Zolotas, A. C., Wang, J., & Goodall, R. M. (2008). Reduced-order robust tilt control design for high-speed railway vehicles. *Vehicle System Dynamics*, *46*(1), 995–1011.

Appendices

A.1 Appendix 1. Vehicle Modelling

Note that (t) has been dropped for simplicity.

A.1.1 Equation of motion for vehicle body (lateral and roll)

$$\begin{aligned} m_v\ddot{y}_v = &-2k_{sy}(y_v - h_1\theta_v - y_b - h_2\theta_b) \\ &- 2c_{sy}(\dot{y}_v - h_1\dot{\theta}_v - \dot{y}_b - h_2\dot{\theta}_b) \\ &- \frac{m_v v^2}{R} + m_v g\theta_0 - h_{g1}m_v\ddot{\theta}_0 \end{aligned} \tag{A1}$$

$$\begin{aligned} i_{vr}\ddot{\theta}_v = &-k_{vr}(\theta_v - \theta_b - \delta_t) \\ &+ 2h_1[K - sy(y_v - h_1\theta_v - y_b - h_2\theta_b) + c_{sy}(\dot{y}_v - h_1\dot{\theta}_v)] \\ &\cdots + m_v g(y_v - y_b) + 2d_1[-k_{az}(d_1\theta_v - d_1\theta_b) \\ &- k_{sz}(d_1\theta_v - d_1\theta_r)] - i_{vr}\ddot{\theta}_0. \end{aligned} \tag{A2}$$

A.1.2 Equation of motion for vehicle bogie(lateral and roll)

$$\begin{aligned} m_b\ddot{y}_b = &\, 2k_{sy}(y_v - h_1\theta_v - y_b - h_2\theta_b) \\ &- 2c_{sy}(\dot{y}_v - h_1\dot{\theta}_v - \dot{y}_b - h_2\dot{\theta}_b) \\ &\cdots - 2k_{py}(y_b - h_3\theta_b - y_w) - 2_{cpy}(\dot{y}_b - h_3\dot{\theta}_b - \dot{y}_w) \\ &- \frac{m_b v^2}{R} + m_b g\theta_0 - h_{g2}m_b\ddot{\theta}_0 \end{aligned} \tag{A3}$$

$$\begin{aligned} i_{br}\ddot{\theta}_b = &\, k_{vr}(\theta_v - \theta_b - \delta_a) + 2h_2[k_{sy}(y_v - h_1\theta_v - y_b - h_2\theta_b) \\ &+ c_{sy}(\dot{y}_v - h_1\dot{\theta}_v - \dot{y}_b - h_2\dot{\theta}_b)] \\ &\cdots - 2d_1[-k_{az}(d_1\theta_v - d_1\theta_b) - k_{sz}(d_1\theta_v - d_1\theta_r)] \\ &+ 2d_2(-d_2k_{pz}\theta_b - d_2c_{pz}\dot{\theta}_b) \\ &\cdots + 2h_3[k_{py}(y_b - h_3\theta_b - y_w) \\ &+ c_{py}(\dot{y}_b - h_3\dot{\theta}_b - \dot{y}_w)] - i_{br}\ddot{\theta}_0. \end{aligned} \tag{A4}$$

A.1.3 Dynamics of air spring state

$$\theta_r = -\frac{k_{sz} + k_{rz}}{c_{rz}}\theta_r + \frac{k_{sz}}{c_{rz}}\theta_v + \frac{k_{rz}}{c_{rz}}\theta_b + \dot{\theta}_b. \tag{A5}$$

A.1.4 Dynamics of ARB actuation system

$$\ddot{\delta}_t = -22\dot{\delta}_t - 483.6\delta_t + 483.6\delta_{t_i}. \tag{A6}$$

A.1.5 Bogie kinematics

$$\ddot{y}_w = -12.57\dot{y}_w - 987y_w + 987y_0. \tag{A7}$$

A.2 Appendix 2. P_{CT} factor

P_{CT} factor formula: $P_{CT} = (A\ddot{y} + B\dddot{y} - C)_{\geq 0} + D\dot{\theta}^E$.

With the constants given below:

Condition	A	B	C	D	E
Standing passengers	2.80	2.03	11.1	0.185	2.283
Seated passengers	0.88	0.95	5.9	0.120	1.626

where (also see Figure A1):

- P_{CT} = passenger comfort index on curve transition, representing the percentage of passengers feeling discomfort
- $\ddot{y}$ = maximum vehicle body lateral acceleration, in the time interval: beginning of the curve transition and 1.6 sec after the end of the transition (expressed in % age of g), g denotes gravity.
- $\dddot{y}$ = maximum lateral jerk level, calculated as the maximum difference between two subsequent values of $\ddot{y}$ no closer than 1sec, in the time interval: 1sec before the start of the curve transition and the end of the transition (expressed in % age of g/sec).
- $\dot{\theta}$ = maximum absolute value of vehicle body roll speed, in the time interval between the beginning of the curve transition to the end of the curve transition (expressed in degrees per second), dot denotes the derivative with respect to time *t*.

A.3 Appendix 3. Variables and parameters list

y_v, y_b, y_0	Lateral displacement of body, bogie and railtrack (m)
$\theta_v, \theta_b, \delta_a$	Roll displacement of body, bogie and actuator (rad)
θ_0	Rail track cant, curve radius (rad)
θ_r	Air spring reservoir roll deflection (rad)
y_w	Bogie kinematics position (m)
v	Vehicle forward speed (tilting: 58 m/s)
m_v	Half body mass, 19,000 kg
i_{vr}	Half body inertia, 25,000 kg m^2
m_b	Bogie mass, 2500 kg
i_{br}	Bogie roll inertia, 1500 kg m^2
k_{az}	Air spring area stiffness, 210,000 N/m
k_{sz}	Air spring series stiffness, 620,000 N/m
k_{rz}	Air spring reservoir stiffness, 244,000 N/m
c_{rz}	Air spring reservoir damping, 33,000 Ns/m
k_{sy}	Secondary lateral stiffness, 260,000 N/m
c_{sy}	Secondary lateral damping, 33,000 Ns/m

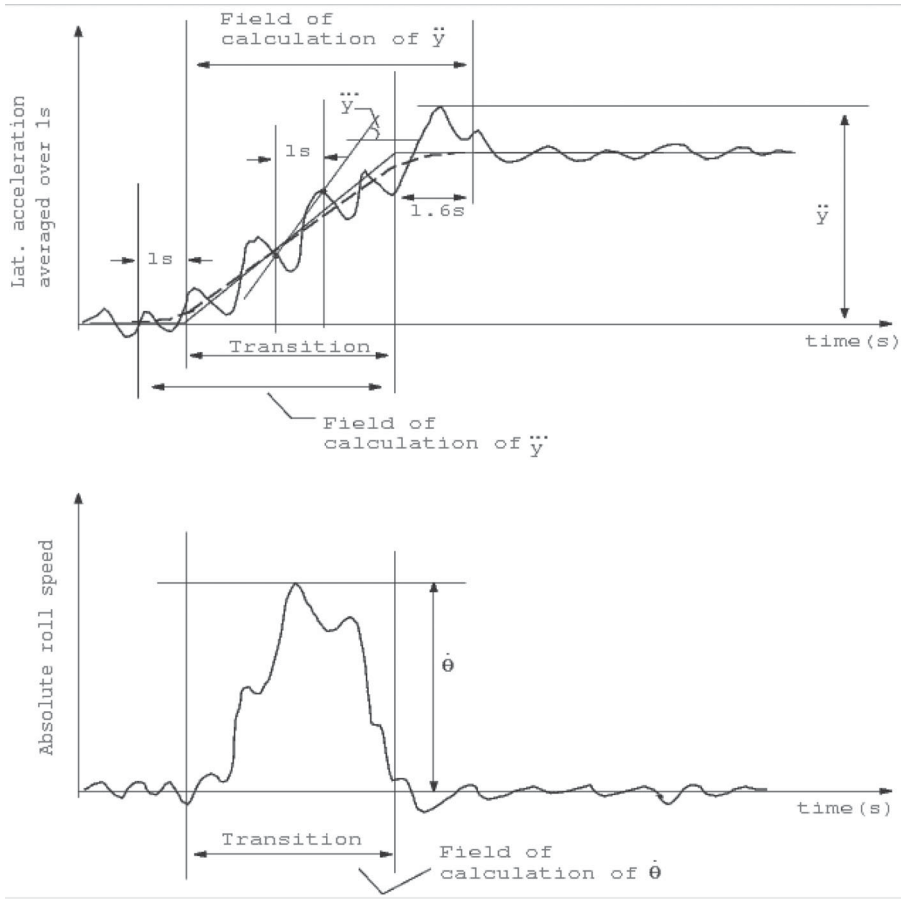

Figure A1. P_{CT} calculations visualization.